https://doi.org/10.5194/os-2020-87
Preprint. Discussion started: 5 November 2020

Ocean Science
Discussions
Open Access
EGU

Assessment of 21 years of Arctic Ocean Absolute Sea Level Trends (1995-2015)

Carsten Ankjær Ludwigsen[1], Ole Baltazar Andersen[1], and Stine Kildegaard Rose[1]

[1]DTU Space, Elektrovej 328, 2800 Kgs. Lyngby, Denmark

Correspondence: Carsten Ankjær Ludwigsen (caanlu@space.dtu.dk)

Abstract. The Arctic Ocean is at the frontier of the fast changing climate in the northern latitudes. As the first study, we assess the different mass and steric components of the observed sea level trend from both absolute sea level (ASL) from altimetry and tide gauges, without using gravimetric observations from GRACE. This approach permits a longer time series and avoids problems with errors from leakage effects in GRACE-products. ASL is equal to mass-driven sea level added with steric sea level, while tide gauge based sea level are also corrected with novel estimates of vertical land movement. Calculations of the mass component from present-day deglaciation, shows that deglaciation rises Arctic sea level with more than 1 mm y^{-1}, while the steric contribution is between -5 and 15 mm y^{-1} with large spatial variability, with the halosteric signal dominating the pattern. A dynamic mass contribution is derived from the Estimating Circulation and Climate of the Oceans (ECCO)-model (version 4 release 4), which varies between -1 and 2 mm y^{-1}. The combined mass and steric product agrees (within uncertainty) with ASL-trends observed from altimetry in 99% of the Arctic, although large uncertainties originate from poor data coverage in the steric data and large variability in the dynamic product. A comparison with ASL trends observed at tide gauges agrees with mass+steric at 11 of 12 tide gauge sites.

1 Introduction

The Arctic is globally the region with the fastest changing climate and is warming twice the rate of the global average. The resulting deglaciation of land and sea ice and ocean freshening all changes the sea level, hence is understanding sea level in the Arctic Ocean paramount for mapping consequences of climate change.

Spatial assessments of the sea level budget of the Arctic has in previous studies shown to be difficult (Henry et al., 2012; Armitage et al., 2016; Carret et al., 2017; Ludwigsen and Andersen, 2020; Raj et al., 2020), because both satellite observations and in-situ observations are less consistent than in low and mid-latitudes and challenged by the Arctic environment and fast-changing climate. Observations from the Gravity Recovery And Climate Experiment (GRACE) offer the only direct Arctic-wide measurements of the mass component, but discrepencies of over 10 mm y^{-1} (Ludwigsen and Andersen, 2020) exist among different GRACE-products (Wiese et al., 2016; Save et al., 2016; Luthcke et al., 2013), and previous studies often choose the solution that fits the altimetric results (Carret et al., 2017; Raj et al., 2020). A cross-comparison of different combinations of GRACE, steric products and altimetry (Ludwigsen and Andersen, 2020), showed that the Arctic sea level budget using an

https://doi.org/10.5194/os-2020-87
Preprint. Discussion started: 5 November 2020

interpolated DTU steric product and a mass-product from the GRACE-satellites (GRACE JPL mascons (Wiese et al., 2016)) for 2003 to 2015 agreed well spatially with an altimetry-product from CPOM (Armitage et al., 2016).

Changes in absolute sea level (ASL) can be divided into two main contributions; changed water column density due to changes in salinity or temperature, which is called *steric change* and *mass change* (also called Ocean Bottom Pressure) due to changes of the gravitational field, land-to-ocean water mass flux and dynamic changes from changing wind stress and atmospheric pressure.

$$\dot{\mathrm{ASL}} = \dot{\mathrm{Steric}} + \dot{\mathrm{Mass}} \tag{1}$$

Tide gauges (TG) gives direct measurements of sea level relative to the solid earth - called relative sea level (RSL). ASL measured by satellite altimetry is measured relative to the Earth's center. The difference between ASL and RSL is defined by the deformation of the solid Earth - called vertical land movement (VLM).

$$\mathrm{ASL} = \mathrm{RSL} + \mathrm{VLM} \tag{2}$$

Bypassing GRACE makes it possible to extend the time series to 21 years from 1995-2015, which generally is 8 years more than assessments using GRACE (Armitage et al., 2016; Carret et al., 2017; Raj et al., 2020) which was first launched in mid 2002. This has the advantage, that non-secular and non-seasonal effects of the Arctic Oscillation, which tends to dominate the dynamic mass contribution (Henry et al., 2012; Armitage et al., 2018) gets smaller.

2 Altimetry

The DTU/TUM Arctic altimetric dataset (Rose et al., 2019) provides an independent estimate of ASL change. For the 1995-2015 period, both ERS-1, ERS-2, Envisat (limited to 81.5°N) and Cryo-Sat-2 (limited to 88°N) is used. It combines results of different retrackers as well as conventional and SAR-altimetry, which may lead to biases (Rose et al., 2019). In particular ERS-1/2 has a relative low spatial resolution and thereby limiting the measurements from leads (open-ocean inbetween the sea ice floes) in sea ice. Also difficulties to distinguish between melt ponds on top of the sea ice and leads were shown to be difficult. The used DTU altimetry product is not corrected for IB and is spatially limited southward to 65°N. The altimetric sea level trend is shown in the right map of figure 5.

3 Tide Gauge data

Tide gauges with a consistent time series are few and unevenly distributed in the Arctic (Henry et al., 2012; Limkilde Svendsen et al., 2016). Locations with both TG and GNSS to measure VLM is even rarer. As a substitute for GNSS-measurements, we correct TG with the VLM-model described in (Ludwigsen et al., 2020a), which offers accurate VLM predictions for the Arctic area.

Twelve TG's are selected in the Arctic region from the PSMSL-database (Holgate et al., 2012) (displayed in figure 1). The selection is based on visual inspection of the monthly time series and to ensure that as many regions of the Arctic is

https://doi.org/10.5194/os-2020-87
Preprint. Discussion started: 5 November 2020

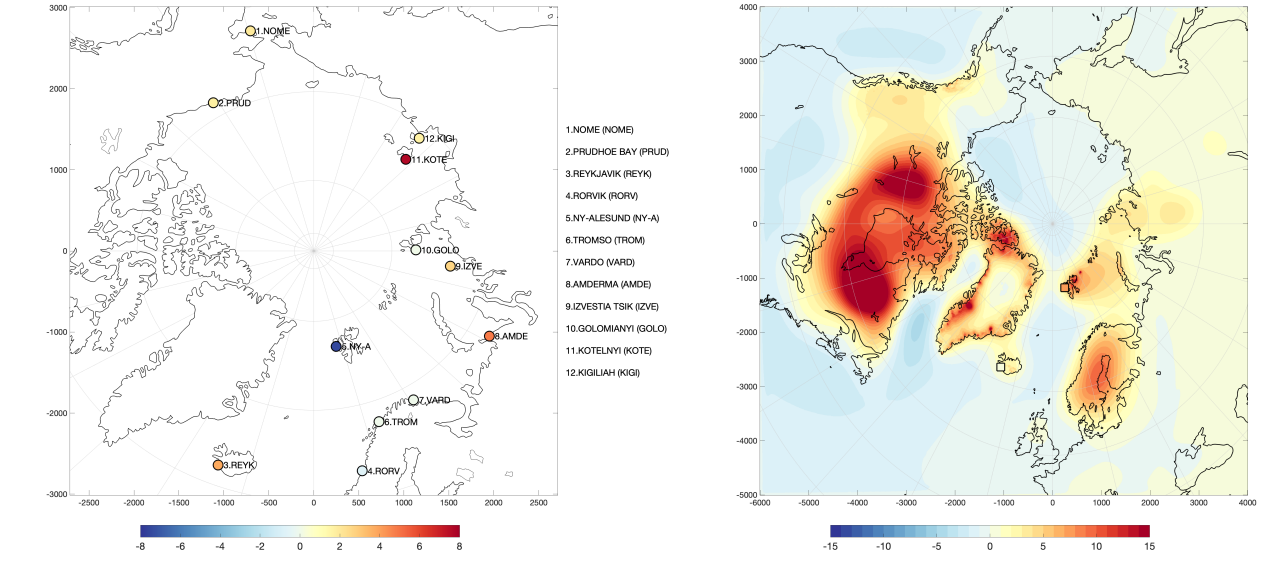

Figure 1. Left: 1995-2015 RSL trend [mm y^{-1}] and location of the selected tide gauges of this study. Right: 1995-2015 VLM-trend [mm y^{-1}] from the model of Ludwigsen et al. (2020b). The VLM-trend from the GNSS-sites at Reykjavik and Ny-Ålesund is shown with squared markers.

represented as possible. A 3-month averaged time series from 1995-2015 of every TG and the linear trend is shown in figure 2 and is corrected for VLM by using the VLM-model (Ludwigsen et al., 2020b) or, as in the case for Ny-Alesund and Reykjavik, using nearby GNSS for VLM (see figure 1). Reykjavik (64.2°N), Nome (64.5°N), and Rorvik (64.9°N) are located off the edge of the DTU/TUM Arctic altimetry dataset (Rose et al., 2019), which only extends to 65°N, but are nevertheless included to extend the spatial distribution of the TG-sites.

TG-trends are determined with least-squares method using months with data between 1995 and 2015 and the VLM-correction is interpolated onto the monthly TG-time series. From figure 2, we see that trends in the Arctic vary with nearly +/- 1 cm y^{-1}, with Ny-Ålesund on Svalbard having a negative sea level trend of -7.45 mm y^{-1}, while Kostelnyi Island between the Laptev and East Siberian Sea shows a positive trend of 7.67 mm y^{-1}.

The VLM-model utilizes the Caron2018 GIA-model (Caron et al., 2018) which is added to an annual elastic VLM-model from 1995-2015 change in present-day ice loading (PDIL). As shown in Ludwigsen and Andersen (2020), Ny-Ålesund and Reykjavik experience extraordinary VLM, caused by substantial deglaciation during the Little Ice Age (Svalbard) and low mantle viscosities (Iceland and Greenland), that is not restored in the VLM-model. Therefore, are the two sites corrected with nearby GNSS instead of the VLM-model. GNSS is uncertain at Prudhoe Bay, where it measures a significant subsidence, that is significantly different from the VLM-model. This is probably caused by near-by construction or oil depletion sites. However, the tide gauge is located on a peninsula reaching into the Beaufort Sea 10 km away from the GNSS-location, which is why the VLM-model is trusted over the GNSS-measurement.

https://doi.org/10.5194/os-2020-87
Preprint. Discussion started: 5 November 2020

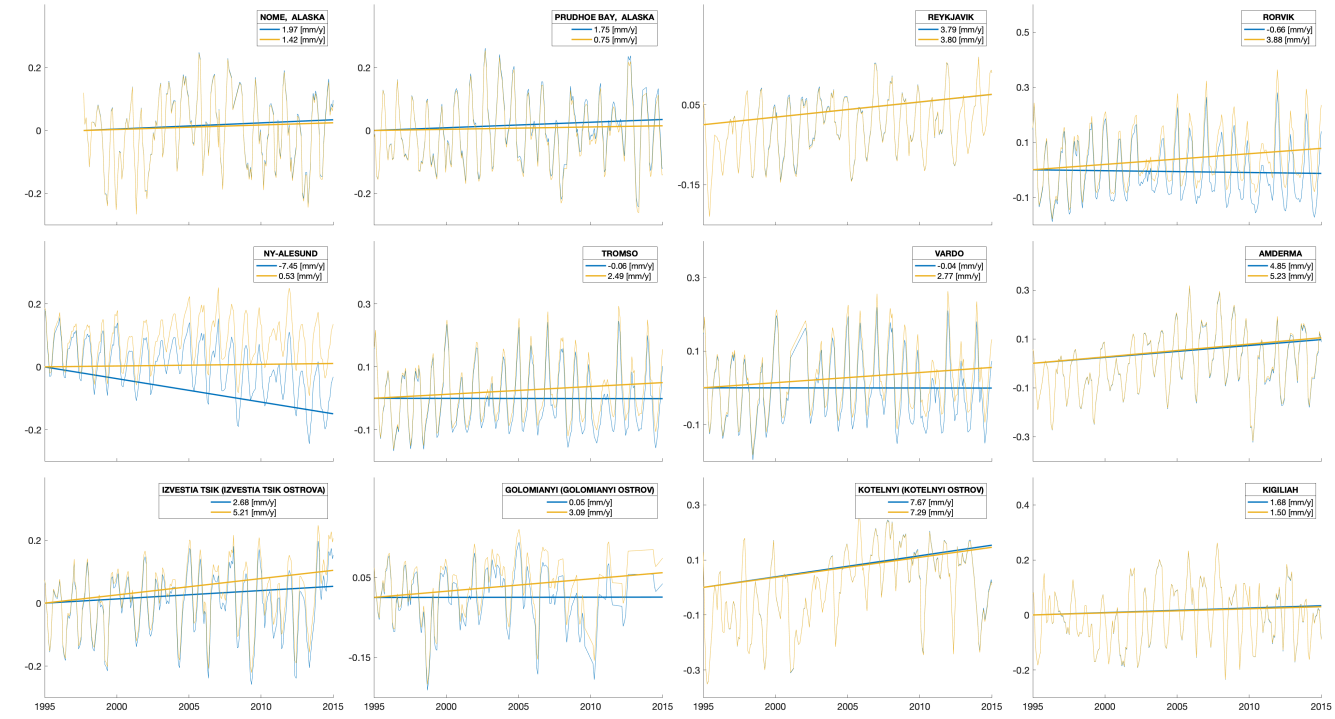

Figure 2. Relative sea level [m] from 1995-2015 registered at the 12 tide gauge from the PSMSL-database (Holgate et al., 2012)]. Blue line represents the 3-month running average, while the thick line is the linear trend (trend estimate [mm y^{-1}] shown in legend). Yellow line represents the absolute sea level and trend, equal to the blue line corrected for VLM with a VLM-model (Ludwigsen et al., 2020b) (except Ny-Ålesund and Reykjavik that are corrected with GNSS).

4 Steric contribution

The DTU steric sea level change is computed as described in Ludwigsen and Andersen (2020). Salinity and temperature measurements from buoys, ice-tethered profiles and ship expeditions in the Arctic Ocean are spatial and temporal unevenly distributed and also depends on seasonal accessibility (Behrendt et al., 2017). Especially, the data density is poor in the shallow seas along the Siberian Coast (Ludwigsen and Andersen, 2020), which is cause to large uncertainties. Temperature and salinity data are interpolated by kriging into a monthly 50x50 km spatial grid on 41 depth levels. If values are more than 3σ away from the mean of neighbouring grid cells, values from the same month in adjacent years is used.

Following the notion of Gill and Niller (1973); Stammer (1997); Calafat et al. (2012); Ludwigsen and Andersen (2020), the change in steric heights, η, are calculated as the sum of halosteric heights (the contribution from salinity change), η_S and thermosteric heights, η_T.

$$\dot{\eta} = \dot{\eta}_S + \dot{\eta}_T \tag{3}$$

https://doi.org/10.5194/os-2020-87
Preprint. Discussion started: 5 November 2020

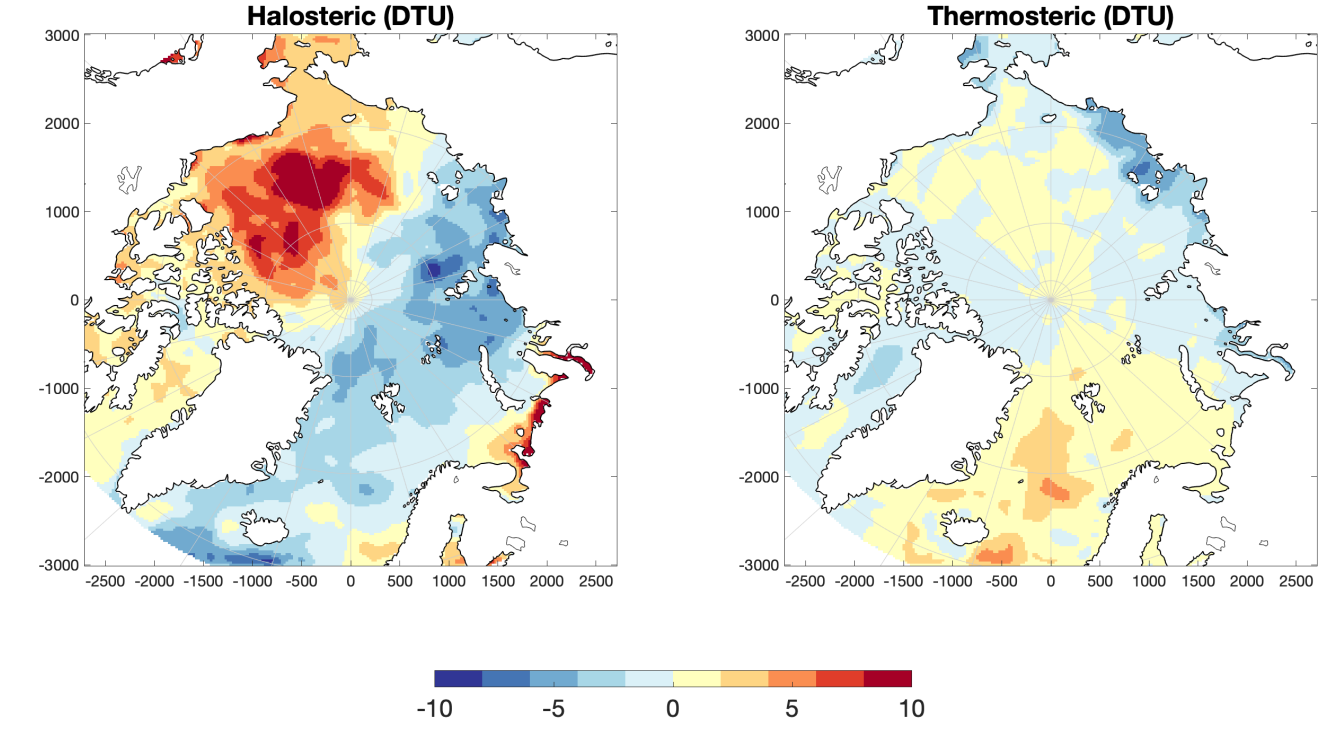

Figure 3. Halo- and thermosteric sea level trend [mm y^{-1}] from 1995-2015 derived from the DTU product which was used in Ludwigsen and Andersen (2020).

Depth profiles from the temperature and salinity grids are used for computing the right-hand side of equation 3:

$$\eta_S = -\frac{1}{\rho_0}\int_{-H}^{0} \beta S' dz \tag{4}$$

$$\eta_T = \frac{1}{\rho_0}\int_{-H}^{0} \alpha T' dz \tag{5}$$

where H denotes the minimum height (maximum depth (z)). S' and T' are defining salinity and temperature anomalies, with reference values used in Ludwigsen and Andersen (2020) are 0 C°and 35psu. β is the saline contraction coefficient and α is the thermal expansion coefficient. The opposite sign of η_S is needed since β represents a contraction (opposite to thermal expansion). α and β are functions of absolute salinity, conservative temperature and pressure, and is determined with help from the freely available TEOS-10 software (Roquet et al., 2015). Map of $\dot{\eta}_S$ and $\dot{\eta}_T$ from 1995-2015 is shown in figure 3.

https://doi.org/10.5194/os-2020-87
Preprint. Discussion started: 5 November 2020


Ocean Science Discussions

5 Mass contribution

Maps of the individual contributions to change in ocean mass is shown in figure 4. We divide the mass contributions into changes caused by changes in surface loading $\dot{N}$, from Greenland $\dot{N}_{GRE}$, Northern Hemisphere glaciers $\dot{N}_{GNH}$, Antarctica $\dot{N}_{ANT}$ and GIA $\dot{N}_{GIA}$, and atmospheric pressure (IB) and a dynamic contribution ($D\dot{M}$).

$$\dot{\text{Mass}} = \dot{N}_{GRE} + \dot{N}_{GNH} + \dot{N}_{ANT} + \dot{N}_{GIA} + I\dot{B} + D\dot{M} \tag{6}$$

Similar to the VLM-product (Ludwigsen et al., 2020a), the Regional Elastic Rebound Calculator (REAR) (Melini et al., 2015) is used to estimate elastic gravitational changes, $\dot{G}$, while gravitational changes from GIA is derived from the Caron2018-model. $\dot{N}$ is retrieved by adding the spatially constant c to the change of the geoid, $\dot{G}$,

$$\dot{N} = \dot{G} + c \tag{7}$$

c is equal to the contribution to global mean sea level (Spada, 2017), and is defined as

$$c = -\frac{M_I \rho_w}{A_O} - \left\langle G - U \right\rangle \tag{8}$$

The used ice model with mass M_I, is a combined high resolution model for glacial estimates (Marzeion et al., 2012; Ludwigsen et al., 2020a) and Greenland ice caps and is here an extended version of the model used for calculations of VLM, U, in (Ludwigsen et al., 2020a). A_O is the global area of the ocean, while ρ_w is the average density of ocean water. $\left\langle ... \right\rangle$, denotes the average of the ocean surface.

The geoid perturbation of non-tidal ocean loading (NOL) (van Dam et al., 2012) and rotational feedback (RF) (King et al., 2012) is not shown since it is below 0.05 mm y^{-1}, but is included in $\dot{N}_{GNH}$. The change in surface mass, M_I, is zero for GIA, RF and NOL. The GIA contribution to global mean sea level (c) is 0.3 mm y^{-1} consistent with other studies (Peltier, 2009; Spada, 2017).

Inverse Barometer (IB) is estimated by the simple relationship derived from the hydro-static equation (Naeije et al., 2000; Pugh and Woodworth, 2014). Monthly averaged pressure estimates from National Center for Environmental Prediction (NCEP) are used for the change in surface pressure Δp:

$$\text{IB} = -9.948 \text{ [mm/mbar]} \, \Delta p \tag{9}$$

Figure 4 also shows the mass-trends derived from Estimating the Circulation and Climate of the Ocean (ECCO) version 4 release 4 (Forget et al., 2015; Fukumori et al., 2019), which is used to estimate the dynamic contribution to sea level. The dynamic mass change is mainly a wind-driven effect that significantly changes the spatial distribution of ocean mass (Calafat et al., 2012; Dangendorf et al., 2014; Armitage et al., 2018) - also on secular time scales.

Because the ECCO-model is among other forced by wind (Forget et al., 2015), we use the difference between ECCO and the sum of $\dot{N}$ and IB as an estimate of the dynamic contribution to mass ($D\dot{M}$, bottom right map of figure 4).

https://doi.org/10.5194/os-2020-87
Preprint. Discussion started: 5 November 2020

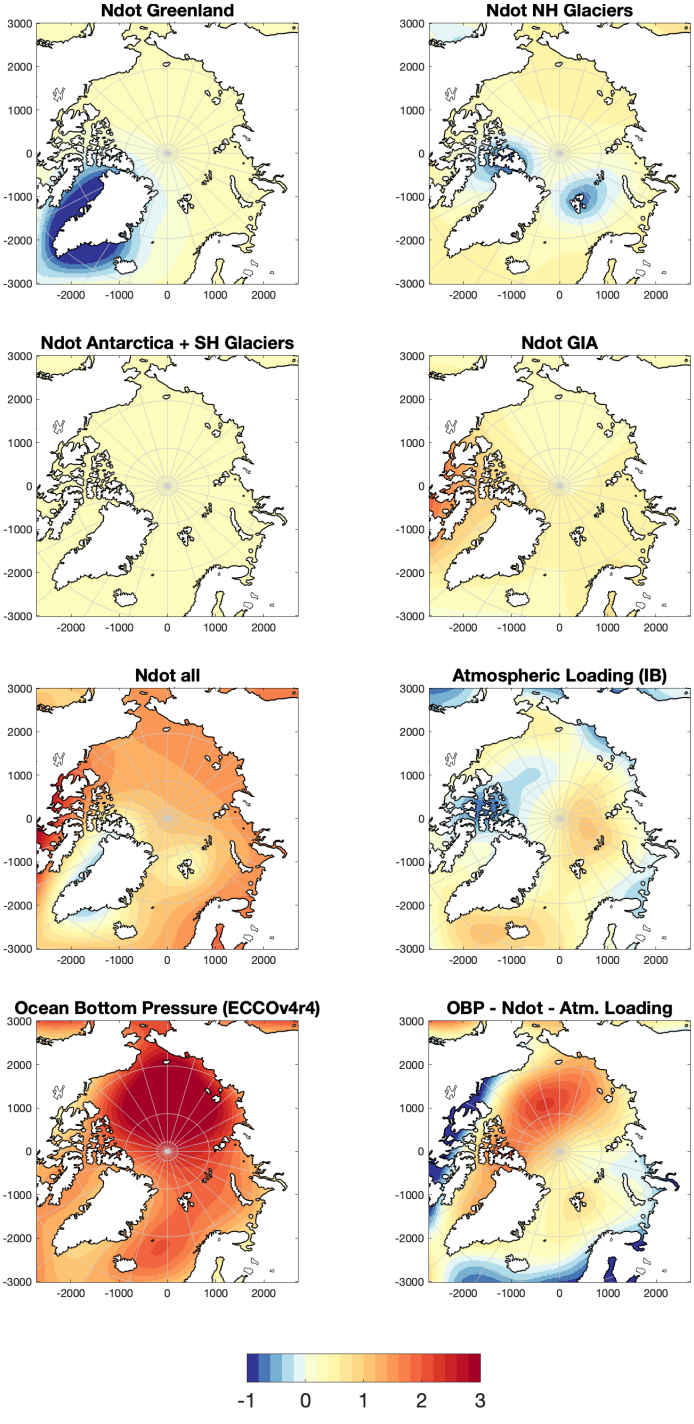

Figure 4. Mass contributions to Arctic Sea Level [mm y^{-1}] from 1995-2015. The top four maps shows the geoid pertubations (Ndot/$\dot{N}$) due to changes in surface mass loading or ocean bottom changes. Third row left is the sum of the top four maps. Right is atmospheric loading or Inverse Barometer (IB). Bottom left is the modeled ocean bottom pressure from ECCO and left is the difference between OBP and Ndot + atm. loading from third row.

https://doi.org/10.5194/os-2020-87
Preprint. Discussion started: 5 November 2020

Ocean Science
Discussions
Open Access
EGU

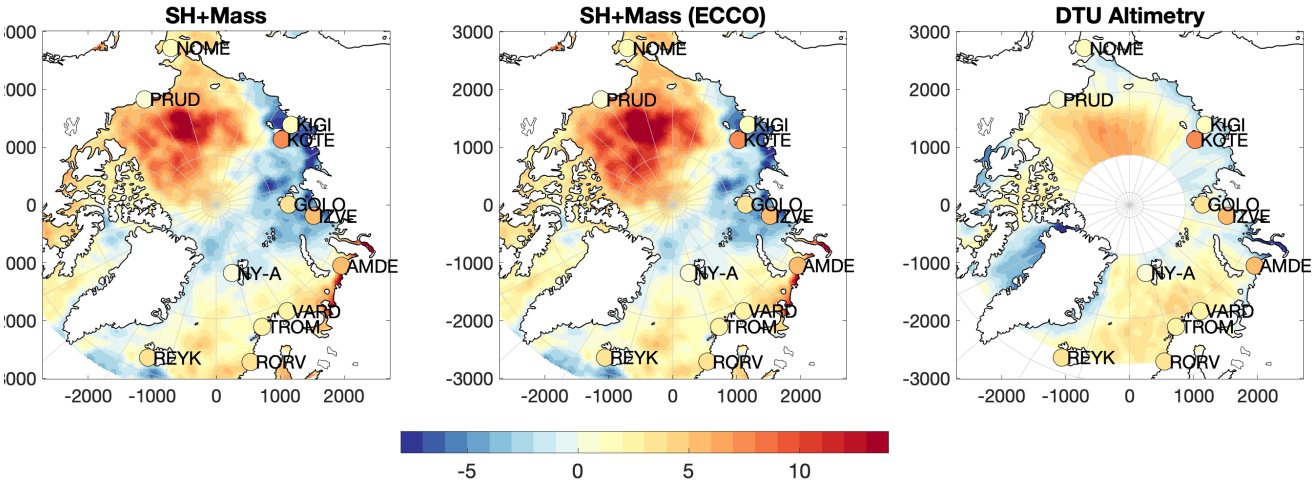

Figure 5. Absolute sea level trend from 1995-2015 [mm y^{-1}]. Left shows pertubation of the geoid + steric contribution, in the middle is OBP from ECCO combined with steric and right is altimetric sea level from Rose et al. (2019). The circles indicate the absolute sea level trend of tide gauges.

6 Comparison of estimates of the Arctic Absolute Sea Level Trend

Two derived trend estimates of the ASL budget is created from steric + mass ($\dot{\eta}$ + $\dot{N} + I\dot{B}$) (without the dynamic component) and steric + mass (ECCO), where ECCO is used as the mass component and hence includes dynamic mass changes. They are compared to the independent estimates of ASL change from TG corrected for VLM and altimetry.

The two derived ASL-trend estimates are shown in figure 5. Since ECCO is partly assimilated with altimetry, only the mass contribution without the dynamic component is truly independent from altimetry. On the scale shown in figure 5, we see that the differences are hardly recognizable.

Because of the sea ice bias before the launch of CryoSat-2 in end-2010, the values before 2011 are likely to be overestimated, which results in a 'flattening' of the trend. In particular, this seems to be the case in the Beaufort Sea (see figure 5), where altimetry and the derived mass+steric product agree on the spatial extent of the dooming of the Beaufort Gyre, but altimetry is 5 mm y^{-1} lower than the mass + steric estimate. Another altimetry product from Armitage et al. (2016) has a larger trend in the Beaufort Gyre in alignment with the steric+mass products.

In the altimetric product a positive sea level trend extends in the Norwegian Sea until it reaches the average sea ice boundary, which (intentionally) coincides with the SAR-boundary of CryoSat-2. From altimetry it is unclear if this signal is a real physical signal or due to bias when different satellites and sea ice and open ocean regions are aligned in the DTU/TUM product. We see from the derived mass+steric product, that some of the positive sea level trends are restored in the Norwegian Sea by the

https://doi.org/10.5194/os-2020-87
Preprint. Discussion started: 5 November 2020

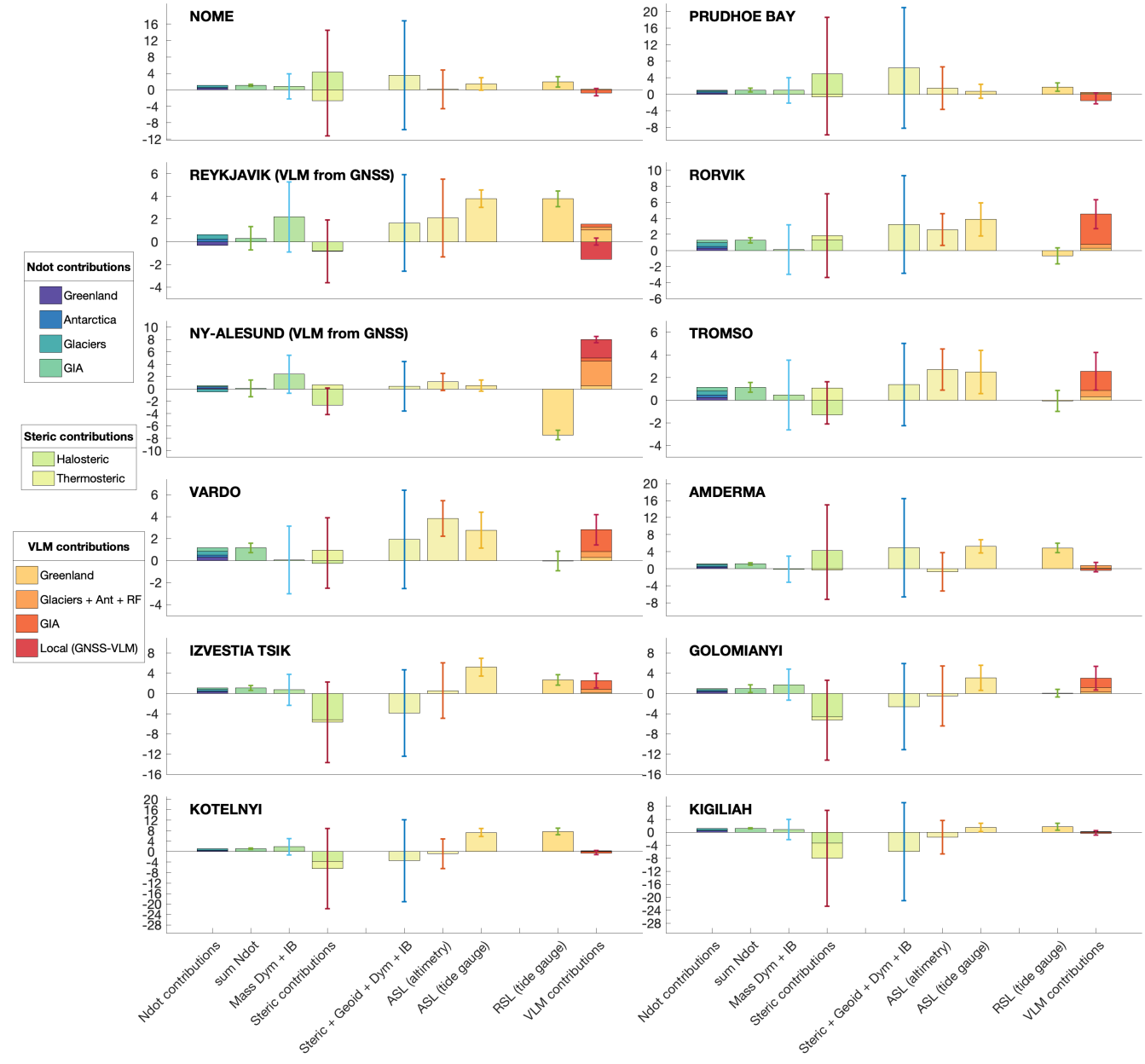

Figure 6. Components of sea level trend [mm y^{-1}] for each tide gauge from 1995-2015. The three bars in the middle (Steric+geoid+dyn, ASL (altimetry) and ASL (tide gauge)) are independent estimates of absolute sea level. The errorbars indicate one standard error (combined error from each component when relevant). The VLM component 'Local (GNSS-VLM)' is only relevant at Reykjavik and Ny Ålesund, because significant local properties causes VLM that is not present in the VLM-model (Ludwigsen et al., 2020b). Glacier component of VLM includes the effect of rotational feedback, ocean loading, and Antarctica which are less than 0.5 mm y^{-1} combined.

https://doi.org/10.5194/os-2020-87
Preprint. Discussion started: 5 November 2020

Ocean Science
Discussions
Open Access
EGU

	TG RSL	VLM	**TG ASL**	Mass ($\dot{N}$)	Mass (IB)	Mass (Dyn)	Steric	**Mass+Steric**	**Altimetry**
NOME	2.0 ± 1.3	-1.0 ± 0.9	**0.9 ± 1.5**	1.1 ± 0.3	0.1	0.8 ± 3.4	1.7 ± 12.9	**3.6 ± 13.2**	**0.1 ± 4.7**
PRUDHOE BAY	1.7 ± 1.0	-1.3 ± 1.3	**0.4 ± 1.6**	1.0 ± 0.8	0.4	1.0 ± 2.8	4.4 ± 14.2	**6.4 ± 14.6**	**1.5 ± 5.2**
REYKJAVIK	3.8 ± 0.7	0.0 ± 0.3	**3.8 ± 0.8**	0.3 ± 1.3	1.0	2.2 ± 4.6	-0.8 ± 2.8	**1.7 ± 4.3**	**2.1 ± 3.4**
RORVIK	-0.7 ± 1.0	4.4 ± 1.8	**3.8 ± 2.1**	1.3 ± 0.3	0.3	0.1 ± 2.9	1.9 ± 5.2	**3.2 ± 6.1**	**2.6 ± 2.0**
NY-ALESUND	-7.4 ± 0.8	8.0 ± 0.5	**0.5 ± 0.9**	0.1 ± 1.4	0.6	2.4 ± 4.0	-2.0 ± 2.2	**0.4 ± 4.0**	**1.1 ± 1.4**
TROMSO	-0.1 ± 0.9	2.4 ± 1.7	**2.4 ± 1.9**	1.1 ± 0.5	0.1	0.5 ± 3.2	-0.2 ± 1.9	**1.4 ± 3.6**	**2.7 ± 1.8**
VARDO	-0.0 ± 0.9	2.7 ± 1.4	**2.7 ± 1.6**	1.2 ± 0.5	-0.1	0.1 ± 2.9	0.7 ± 3.2	**1.9 ± 4.5**	**3.8 ± 1.6**
AMDERMA	4.9 ± 1.1	0.4 ± 1.1	**5.2 ± 1.6**	1.1 ± 0.3	-0.1	-0.1 ± 3.0	3.9 ± 11.1	**4.9 ± 11.5**	**-0.7 ± 4.5**
IZVESTIA TSIK	2.7 ± 1.0	2.4 ± 1.5	**5.1 ± 1.8**	1.1 ± 0.6	0.2	0.7 ± 4.4	-5.7 ± 8.0	**-3.9 ± 8.6**	**0.6 ± 5.5**
GOLOMIANYI	0.0 ± 0.8	2.9 ± 2.3	**2.9 ± 2.5**	0.9 ± 0.9	0.6	1.7 ± 4.4	-5.3 ± 7.9	**-2.6 ± 8.5**	**-0.5 ± 5.9**
KOTELNYI	7.7 ± 1.3	-1.0 ± 0.8	**6.6 ± 1.5**	1.1 ± 0.2	0.2	1.9 ± 3.6	-6.5 ± 15.3	**-3.5 ± 15.6**	**-0.8 ± 5.6**
KIGILIAH	1.7 ± 1.1	-0.8 ± 0.7	**0.8 ± 1.3**	1.2 ± 0.2	-0.1	0.9 ± 3.1	-8.0 ± 14.8	**-5.9 ± 15.1**	**-1.5 ± 5.1**

Table 1. 1995-2015 sea level trends [mm y^{-1}] of each contribution at the 12 tide gauge locations. The values (except VLM) represent a 100 km radius around the tide gauge. For VLM a 5 km radius is used and for Ny-Alesund and Reykjavik, VLM is taken from GNSS. The columns in bold indicate the estimates of Absolute Sea Level (ASL).

thermosteric contribution (figure 3), thus is a warming of the ocean cause to sea level rise in the region. The boundary between sea ice and open ocean is however less significant.

Obviously, does tide gauges only measure sea level in coastal areas, and therefore not useful when analyzing spatial sea level trend patterns of the Arctic Ocean. Furthermore, is the coastal location often disturbed by the local environment that might be unknown (e.g. small river outflow, local construction, packing of sea ice etc.), which can influence both sea level measurements from tide gauge and altimetry.

In figure 6 and table 1, we quantify the contributions to sea level change explained in this chapter at each of the 12 tide gauge locations using a surrounding average of 100 km radius (5 km for GIA and elastic VLM). This radius ensures, that Rorvik, Nome and Reykjavik reaches the altimetric data, but few data points, might cause the data to be more variable and hence increase the uncertainty.

The Norwegian tide gauges (Rorvik, Tromso, Vardo) are considered the most stable. The derived product is in good agreement with the tide gauge and has for Tromso and Vardo better alignment with the TG-data than altimetry. This is also the region with highest density of hydrographical data and thus most reliable. We see that for Vardo and Rorvik, the sea level change is split between a steric and mass contribution of roughly the same size, which is similar to the share of the global sea level trend (Church and White, 2011; Group, 2018). At Tromso a negative halosteric signal (more saline water) is lowering the sea level trend.

Along the Siberian coast, multiple river outlets contributes to a freshening of the Arctic Ocean (Morison et al., 2012; Armitage et al., 2016), which is reflected by the positive halosteric trend. At Amderma TG, which is located on the coast between the Barents and Kara Sea, there is however no nearby major river outlet, but a significant halosteric signal is still present which

https://doi.org/10.5194/os-2020-87
Preprint. Discussion started: 5 November 2020

matches the tide gauge-measured sea level. Ice loss from Novaya Zemlya contributes with over 1 gigaton of freshwater to the Kara Sea every year (Melkonian et al., 2016), but it is unclear if this is the reason for the halosteric sea level rise at Anderma, or if the halosteric signal is (falsely) extrapolated from the gulf of Ob which has mayor river outlets and the match with tide gauge is accidental. The altimetric signal reflects the mass contribution, which together with low hydrographic data density in the region, could indicate that both the tide gauge and halosteric sea level trends are overestimated.

The four other tide gauges along the Siberian coast all show a pattern, where mass+steric has a negative trend, altimetry has a slight negative or positive trend and the tide gauge has a clear positive trend. Due to poor hydrographic coverage along the Siberian coast (Ludwigsen and Andersen, 2020) it is difficult to estimate the 'true' sea level. The positive trend among tide gauges in the Siberian Seas is however consistent and has been recognized in other studies using an extended set of Siberian tide gauges (Proshutinsky et al., 2004; Henry et al., 2012). Remarkably is that the TG-trend at Kotelnyi and Kigiliah differ with almost 6 mm y^{-1} despite being less than 250 km apart. This difference is only realistic if local circumstances is affecting the RSL.

Nome and Prudhoe Bay in Alaska both show a positive steric trend which is not reflected in sea level trends from altimetry or the tide gauge. The strong halosteric trend of the Beaufort Gyre, might be extrapolated towards the Alaskan coastline. Altimetry agrees reasonably well with the tide gauge trend.

Few hydrographic data around Reykjavik, makes the steric sea level rather uncertain as well. A negative halosteric contribution causes the steric+mass product to be to low compared to TG-data and altimetry.

At Ny-Ålesund on Svalbard, which like the other Norwegian TG-sites has good hydropgraphic data density, is the mass + steric contribution in agreement with the TG-trend. Ny-Ålesund is dominated by a large VLM caused by deglaciation in recent years and after the Little Ice Age that ended in the 19th century (Rajner, 2018; Ludwigsen et al., 2020a). This uplift completely mitigates the large sea level fall measured by the tide gauge. A small mass upward trend is countered by a smaller steric downward trend, which in total agrees with the tide gauge measured sea level trend. Altimetry shows a slightly higher trend.

Generally the largest uncertainties (estimated as standard error of the trend) are found along the Siberian coast and in the interior of the Arctic where the largest sea level trend is present (see figure 7). The steric uncertainty, which in most cases is the largest source of uncertainty, is computed as the standard deviation of the detrended and deseasoned time series, which naturally reflects if steric heights are unstable and poorly constrained. This method requires in principal temporal independence, which is not entirely true, since data from adjacent years are used instead of outliers. Furthermore, large influence by the non-periodic and non-linear Arctic Oscillation, would enhance the uncertainty, even though this is a real physical signal.

The mass contribution and VLM has naturally the largest uncertainties close to glaciated areas. Glacial ice loss on Baffin Island is poorly constrained in the ice model, which is reflected in large uncertainties in this area. A significant uncertainty also originates in the dynamic mass loss, which probably also can be attributed to the Arctic Oscillation, which significantly changes wind patterns. Since no uncertainties are associated with the ECCO-product, we also here assume no temporal correlation, and calculate the standard deviation of the time series, even though the model likely has inter-annual correlations.

https://doi.org/10.5194/os-2020-87
Preprint. Discussion started: 5 November 2020

Ocean Science
Discussions
Open Access
EGU

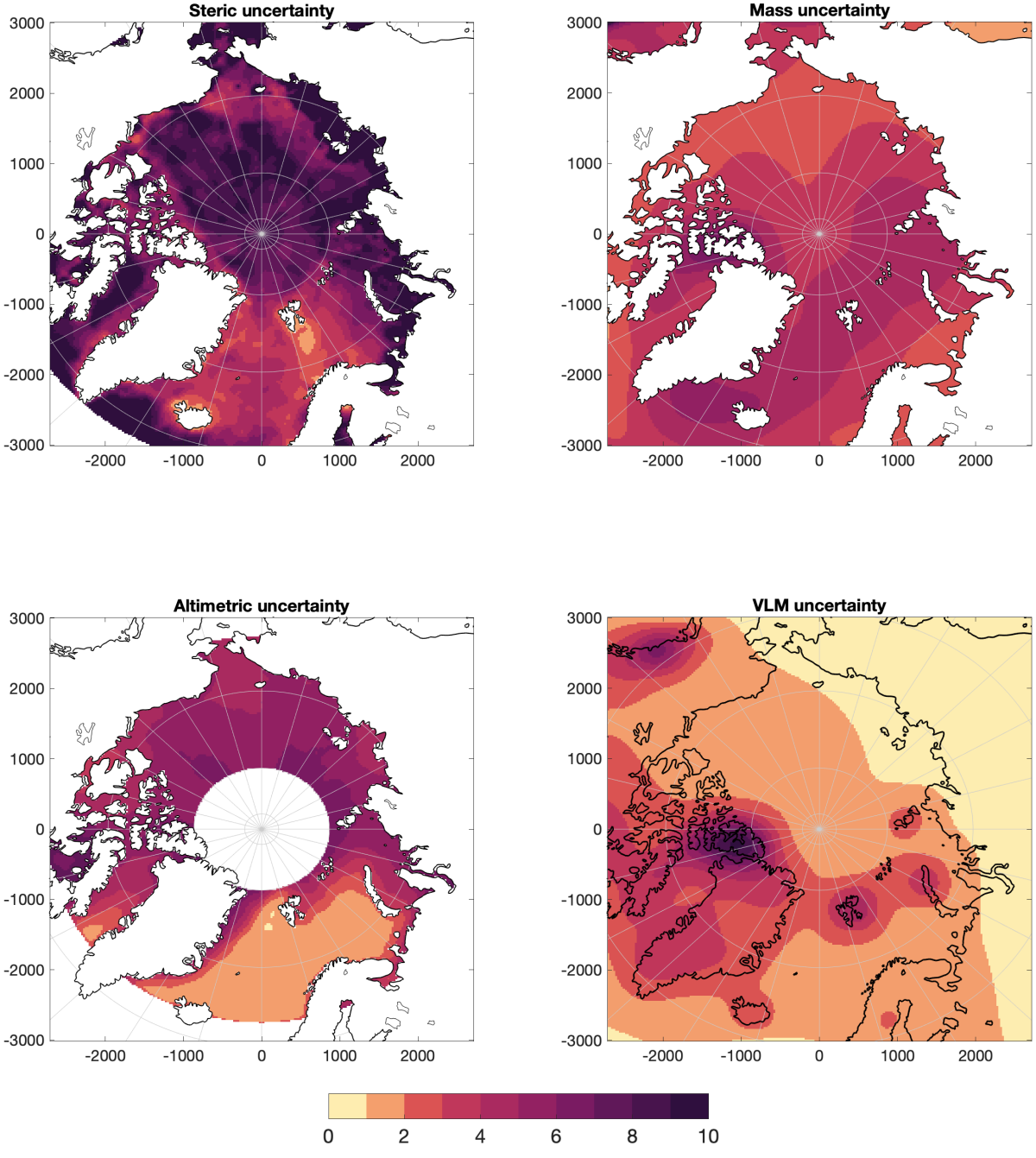

Figure 7. Maps of uncertainty (1 standard error) of the 1995-2015 trend [mm y^{-1}] for combined steric, combined $\dot{N}$ + dynamic mass + IB, altimetry and combined VLM contributions.

https://doi.org/10.5194/os-2020-87
Preprint. Discussion started: 5 November 2020

Ocean Science
Discussions
Open Access
EGU

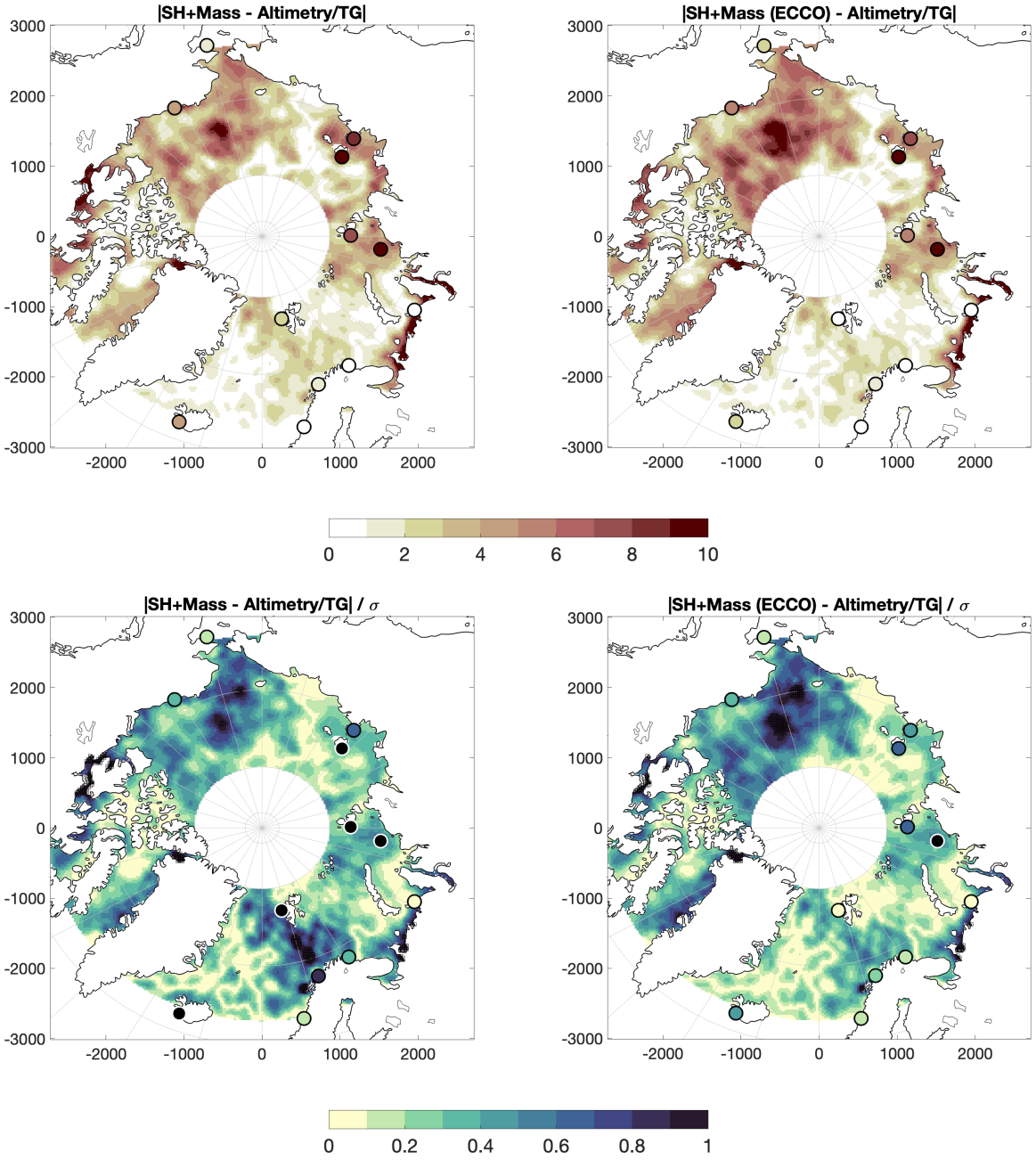

Figure 8. Map in the top row shows the absolute difference between altimetry and the steric+mass (no dynamic contribution) product (left column) and altimetry and the steric+mass from the ECCO-model (right column). Bottom row, shows the absolute difference relative to the combined uncertainty (σ). The dots show the difference to VLM-corrected tide gauges. At the tide gauges marked with black, is the difference larger than the combined uncertainty.

https://doi.org/10.5194/os-2020-87
Preprint. Discussion started: 5 November 2020

7 Conclusion

All significant contributions to the sea level change from 1995-2015 in the Arctic Ocean have been mapped and assessed at 12 tide gauges located throughout the Arctic, without the use of GRACE data or modeled steric data. Thereby are we able to attribute effects on Arctic Sea Level to their origin and thus understand the causes behind the observed sea level trend. By using a VLM-model that includes both GIA and elastic uplift, the TG-data can be utilized in locations if no reliable GNSS-data is present.

From figure 5 we clearly see that the general spatial pattern of altimetry is restored in the derived steric estimate and in the mass product. Figure 6 and 7 shows that steric sea level dominates the spatial variability and is also the main source of uncertainty. Some areas, in particular the Norwegian Sea and more interior of the Arctic Ocean, seems to be rather well constrained and understood from the individual contributions. The Siberian seas, are however poorly constrained and both the steric product, altimetry and tide gauges show large uncertainty. Figure 8 shows the spatial agreement between altimetry/tide gauges and the steric+mass or steric+mass(ECCO) product within the combined uncertainty. Without the use of ECCO, the derived product agrees with altimetry at 98% of the area, while only 5 out of 12 of the TG-data agree with derived product. For the steric+mass(ECCO) product, the products agree at 99% of the area and at 11 out of 12 TG's. The areas of disagreement in the Norwegian Sea can be explained by the very low altimetric uncertainty in the area.

Our results show that the sea level budget is not closed or completely understood everywhere - likely because of poorly constrained steric data and uncertain dynamic contribution. however, from figure 8 we see that the uncertainties are in most of the Arctic significantly larger than the difference between a derived product and altimetry, including most of the Siberian Seas. More precise estimates of both the mass and steric product are necessary to get at complete understanding of what changes Arctic sea level and validate sea level trends observed by altimetry, which is not necessarily more accurate than the derived ASL-estimates.

Code and data availability. Tide gauge sea level timeseries is available at psmsl.org, the VLM-model available at data.dtu.dk/articles/dataset/Arctic_Vertical_Land_Motion_5x5_km, DTU Steric is available at ftp.space.dtu.dk/pub/DTU19/STERIC/, the REAR-software is available at github at github.com/danielemelini/rear.git.

Author contributions. CAL: Method, concept, data analysis and writing. OBA: Concept and editing. SKR: Providing altimetry data, validation and editing.

Competing interests. The authors declare no competing interests.

https://doi.org/10.5194/os-2020-87
Preprint. Discussion started: 5 November 2020

Acknowledgements. The authors want to thank Lambert Caron for creating the Caron2018 GIA-model, available at https://vesl.jpl.nasa.gov/solid-earth/gia/. Special thanks to Danielle Melini for creating the REAR-code (Melini et al., 2015). This research was funded by the EU-INTAROS project (Grant agreement no. 727890) (CAL and OBA) and by the ESA-Climate Change Initiative Sea level budget closure (Expro RFP/3-14679/16/INB) (OBA and SKR).

https://doi.org/10.5194/os-2020-87
Preprint. Discussion started: 5 November 2020

References

Armitage, T. W. K., Bacon, S., Ridout, A. L., Thomas, S. F., Aksenov, Y., and Wingham, D. J.: Arctic sea surface height variability and change from satellite radar altimetry and GRACE, 2003–2014, Journal of Geophysical Research: Oceans, 121, 4303–4322, https://doi.org/10.1002/2015JC011579, https://agupubs.onlinelibrary.wiley.com/doi/abs/10.1002/2015JC011579, 2016.

Armitage, T. W. K., Bacon, S., and Kwok, R.: Arctic Sea Level and Surface Circulation Response to the Arctic Oscillation, Geophysical Research Letters, 45, 6576–6584, https://doi.org/10.1029/2018GL078386, https://agupubs.onlinelibrary.wiley.com/doi/abs/10.1029/2018GL078386, 2018.

Behrendt, A., Sumata, H., Rabe, B., and Schauer, U.: A comprehensive, quality-controlled and up-to-date data set of temperature and salinity data for the Arctic Mediterranean Sea (Version 1.0), links to data files, https://doi.org/10.1594/PANGAEA.872931, https://doi.org/10.1594/PANGAEA.872931, supplement to: Behrendt, A et al. (2017): UDASH - Unified Database for Arctic and Subarctic Hydrography. Earth System Science Data Discussions, 37 pp, https://doi.org/10.5194/essd-2017-92, 2017.

Calafat, F. M., Chambers, D. P., and Tsimplis, M. N.: Mechanisms of decadal sea level variability in the eastern North Atlantic and the Mediterranean Sea, Journal of Geophysical Research: Oceans, 117, https://doi.org/10.1029/2012JC008285, https://agupubs.onlinelibrary.wiley.com/doi/abs/10.1029/2012JC008285, 2012.

Caron, L., Ivins, E. R., Larour, E., Adhikari, S., Nilsson, J., and Blewitt, G.: GIA Model Statistics for GRACE Hydrology, Cryosphere, and Ocean Science, Geophysical Research Letters, 45, 2203–2212, https://doi.org/10.1002/2017GL076644, https://agupubs.onlinelibrary.wiley.com/doi/abs/10.1002/2017GL076644, 2018.

Carret, A., Johannessen, J. A., Andersen, O. B., Ablain, M., Prandi, P., Blazquez, A., and Cazenave, A.: Arctic Sea Level During the Satellite Altimetry Era, Surveys in Geophysics, 38, 251–275, https://doi.org/10.1007/s10712-016-9390-2, https://doi.org/10.1007/s10712-016-9390-2, 2017.

Church, J. A. and White, N. J.: Sea-Level Rise from the Late 19th to the Early 21st Century, Surveys in Geophysics, 32, 585–602, https://doi.org/10.1007/s10712-011-9119-1, https://doi.org/10.1007/s10712-011-9119-1, 2011.

Dangendorf, S., Calafat, F. M., Arns, A., Wahl, T., Haigh, I. D., and Jensen, J.: Mean sea level variability in the North Sea: Processes and implications, Journal of Geophysical Research: Oceans, 119, https://doi.org/10.1002/2014JC009901, https://agupubs.onlinelibrary.wiley.com/doi/abs/10.1002/2014JC009901, 2014.

Forget, G., Campin, J.-M., Heimbach, P., Hill, C. N., Ponte, R. M., and Wunsch, C.: ECCO version 4: an integrated framework for non-linear inverse modeling and global ocean state estimation, Geoscientific Model Development, 8, 3071–3104, https://doi.org/10.5194/gmd-8-3071-2015, https://gmd.copernicus.org/articles/8/3071/2015/, 2015.

Fukumori, I., Wang, O., Fenty, I., Forget, G., Heimbach, P., and Ponte, R. M.: ECCO Version 4 Release 4 Dataset, accessed: 2020-06-25, 2019.

Gill, A. and Niller, P.: The theory of the seasonal variability in the ocean, Deep Sea Research and Oceanographic Abstracts, 20, 141 – 177, https://doi.org/https://doi.org/10.1016/0011-7471(73)90049-1, http://www.sciencedirect.com/science/article/pii/0011747173900491, 1973.

Group, W. G. S. L. B.: Global sea-level budget 1993–present, Earth System Science Data, 10, 1551–1590, https://doi.org/10.5194/essd-10-1551-2018, https://essd.copernicus.org/articles/10/1551/2018/, 2018.

Henry, O., Prandi, P., Llovel, W., Cazenave, A., Jevrejeva, S., Stammer, D., Meyssignac, B., and Koldunov, N.: Tide gauge-based sea level variations since 1950 along the Norwegian and Russian coasts of the Arctic Ocean: Contribution of the steric and mass components,

Journal of Geophysical Research: Oceans, 117, https://doi.org/10.1029/2011JC007706, https://agupubs.onlinelibrary.wiley.com/doi/abs/10.1029/2011JC007706, 2012.

Holgate, S. J., Matthews, A., Woodworth, P. L., Rickards, L. J., Tamisiea, M. E., Bradshaw, E., Foden, P. R., Gordon, K. M., Jevrejeva, S., and Pugh, J.: New Data Systems and Products at the Permanent Service for Mean Sea Level, Journal of Coastal Research, 29, 493–504, https://doi.org/10.2112/JCOASTRES-D-12-00175.1, https://doi.org/10.2112/JCOASTRES-D-12-00175.1, 2012.

King, M. A., Keshin, M., Whitehouse, P. L., Thomas, I. D., Milne, G., and Riva, R. E. M.: Regional biases in absolute sea-level estimates from tide gauge data due to residual unmodeled vertical land movement, Geophysical Research Letters, 39, https://doi.org/10.1029/2012GL052348, https://agupubs.onlinelibrary.wiley.com/doi/abs/10.1029/2012GL052348, 2012.

Limkilde Svendsen, P., Andersen, O. B., and Aasbjerg Nielsen, A.: Stable reconstruction of Arctic sea level for the 1950–2010 period, Journal of Geophysical Research: Oceans, 121, 5697–5710, https://doi.org/10.1002/2016JC011685, https://agupubs.onlinelibrary.wiley.com/doi/abs/10.1002/2016JC011685, 2016.

Ludwigsen, C., Khan, S. A., Andersen, O. B., and Marzeion, B.: Vertical Land Motion from present-day deglaciation in the wider Arctic, Earth and Space Science Open Archive, p. 18, https://doi.org/10.1002/essoar.10502890.1, https://doi.org/10.1002/essoar.10502890.1, 2020a.

Ludwigsen, C. A. and Andersen, O. B.: Contributions to Arctic sea level from 2003 to 2015, Advances in Space Research, https://doi.org/https://doi.org/10.1016/j.asr.2019.12.027, http://www.sciencedirect.com/science/article/pii/S0273117719309275, 2020.

Ludwigsen, C. A., Andersen, O. B., Khan, S. A., and Marzeion, B.: Arctic Vertical Land Motion (5x5 km), https://doi.org/10.11583/DTU.12554489.v1, https://data.dtu.dk/articles/dataset/Arctic_Vertical_Land_Motion_5x5_km_/12554489, 2020b.

Luthcke, S. B., Sabaka, T., Loomis, B., Arendt, A., McCarthy, J., and Camp, J.: Antarctica, Greenland and Gulf of Alaska land-ice evolution from an iterated GRACE global mascon solution, Journal of Glaciology, 59, 613–631, https://doi.org/10.3189/2013JoG12J147, 2013.

Marzeion, B., Jarosch, A. H., and Hofer, M.: Past and future sea-level change from the surface mass balance of glaciers, The Cryosphere, 6, 1295–1322, https://doi.org/10.5194/tc-6-1295-2012, https://www.the-cryosphere.net/6/1295/2012/, 2012.

Melini, D., Spada, G., Gegout, P., and King, M.: REAR: a Regional ElAstic Rebound calculator. User manual for version 1.0, available on–line at: http://hpc.rm.ingv.it/rear., 2015.

Melkonian, A. K., Willis, M. J., Pritchard, M. E., and Stewart, A. J.: Recent changes in glacier velocities and thinning at Novaya Zemlya, Remote Sensing of Environment, 174, 244 – 257, https://doi.org/https://doi.org/10.1016/j.rse.2015.11.001, http://www.sciencedirect.com/science/article/pii/S0034425715301899, 2016.

Morison, J., Kwok, R., Peralta-Ferriz, C., Alkire, M., Rigor, I., Andersen, R., and Steele, M.: Changing Arctic Ocean freshwater pathways, Nature, 481, 66–70, https://doi.org/10.1038/nature10705, https://doi.org/10.1038/nature10705, 2012.

Naeije, M., Schrama, E., and Scharroo, R.: The radar Altimeter Database System project RADS, 2, 487 – 490 vol.2, https://doi.org/10.1109/IGARSS.2000.861605, 2000.

Peltier, W.: Closure of the budget of global sea level rise over the GRACE era: the importance and magnitudes of the required corrections for global glacial isostatic adjustment, Quaternary Science Reviews, 28, 1658 – 1674, https://doi.org/https://doi.org/10.1016/j.quascirev.2009.04.004, http://www.sciencedirect.com/science/article/pii/S0277379109001218, quaternary Ice Sheet-Ocean Interactions and Landscape Responses, 2009.

https://doi.org/10.5194/os-2020-87
Preprint. Discussion started: 5 November 2020

Proshutinsky, A., Ashik, I. M., Dvorkin, E. N., Häkkinen, S., Krishfield, R. A., and Peltier, W. R.: Secular sea level change in the Russian sector of the Arctic Ocean, Journal of Geophysical Research: Oceans, 109, https://doi.org/10.1029/2003JC002007, https://agupubs.onlinelibrary.wiley.com/doi/abs/10.1029/2003JC002007, 2004.

Pugh, D. and Woodworth, P.: Sea-Level Science: Understanding Tides, Surges, Tsunamis and Mean Sea-Level Changes, Cambridge University Press, https://doi.org/10.1017/CBO9781139235778, 2014.

Raj, R. P., Andersen, O. B., Johannessen, J. A., Gutknecht, B. D., Chatterjee, S., Rose, S. K., Bonaduce, A., Horwath, M., Ranndal, H., Richter, K., Palanisamy, H., Ludwigsen, C. A., Bertino, L., Nilsen, J. E. , Knudsen, P., Hogg, A., Cazenave, A., and Benveniste, J.: Arctic Sea level Budget Assessment During the GRACE/Argo Time Period, Remote Sensing, 12, https://doi.org/10.3390/rs12172837, https://www.mdpi.com/2072-4292/12/17/2837, 2020.

Rajner, M.: Detection of ice mass variation using gnss measurements at Svalbard, Journal of Geodynamics, 121, 20 – 25, https://doi.org/https://doi.org/10.1016/j.jog.2018.06.001, http://www.sciencedirect.com/science/article/pii/S0264370718300450, 2018.

Roquet, F., Madec, G., McDougall, T. J., and Barker, P. M.: Accurate polynomial expressions for the density and specific volume of seawater using the TEOS-10 standard, Ocean Modelling, 90, 29 – 43, https://doi.org/https://doi.org/10.1016/j.ocemod.2015.04.002, http://www.sciencedirect.com/science/article/pii/S1463500315000566, 2015.

Rose, S. K., Andersen, O., Passaro, M., Ludwigsen, C., and Schwatke, C.: Arctic Ocean Sea Level Record from the Complete Radar Altimetry Era: 1991-2018, Remote Sensing, 11, https://doi.org/10.3390/rs11141672, 2019.

Save, H., Bettadpur, S., and Tapley, B. D.: High-resolution CSR GRACE RL05 mascons, Journal of Geophysical Research: Solid Earth, 121, 7547–7569, https://doi.org/10.1002/2016JB013007, https://agupubs.onlinelibrary.wiley.com/doi/abs/10.1002/2016JB013007, 2016.

Spada, G.: Glacial Isostatic Adjustment and Contemporary Sea Level Rise: An Overview, Surveys in Geophysics, 38, 153–185, https://doi.org/10.1007/s10712-016-9379-x, https://doi.org/10.1007/s10712-016-9379-x, 2017.

Stammer, D.: Steric and wind-induced changes in TOPEX/POSEIDON large-scale sea surface topography observations, Journal of Geophysical Research: Oceans, 102, 20 987–21 009, https://doi.org/10.1029/97JC01475, https://agupubs.onlinelibrary.wiley.com/doi/abs/10.1029/97JC01475, 1997.

van Dam, T., Collilieux, X., Wuite, J., Altamimi, Z., and Ray, J.: Nontidal ocean loading: amplitudes and potential effects in GPS height time series, Journal of Geodesy, 86, 1043–1057, https://doi.org/10.1007/s00190-012-0564-5, https://doi.org/10.1007/s00190-012-0564-5, 2012.

Wiese, D. N., Landerer, F. W., and Watkins, M. M.: Quantifying and reducing leakage errors in the JPL RL05M GRACE mascon solution, Water Resources Research, 52, 7490–7502, https://doi.org/10.1002/2016WR019344, https://agupubs.onlinelibrary.wiley.com/doi/abs/10.1002/2016WR019344, 2016.